12-1-2002

Analysis Of Doppler-Broadened X-Ray Emission Line Profiles From Hot Stars

David H. Cohen
Swarthmore College, dcohen1@swarthmore.edu

Roban Hultman Kramer , '03

S. P. Owocki

ANALYSIS OF DOPPLER-BROADENED X-RAY EMISSION LINE PROFILES FROM HOT STARS

David H. Cohen [a] Roban H. Kramer [b] Stanley P. Owocki [c]

[a]Swarthmore College, Department of Physics and Astronomy, Swarthmore PA 19081

[b]Swarthmore College, Department of Physics and Astronomy, Swarthmore PA 19081 and Prism Computational Sciences, 455 Science Dr., Madison WI 53711

[c]Bartol Research Institute, University of Delaware, Newark DE 19716

We show how X-ray emission arising within an accelerating, expanding medium that also contains a source of continuum absorption generates line profiles of a characteristic shape. A simple, spherical wind model based on this picture provides good fits to the *Chandra HETGS* spectrum of the prototypical O star, ζ Pup. We discuss the model, the fitting procedure and the determination of confidence limits on the model parameters, and our initial results for this star. The derived fit parameters are consistent with a generic wind-shock scenario for ζ Pup, but there are several surprising aspects of the results, including a lower-than-expected mean wind optical depth and a nearly complete lack of wavelength dependence of the results.

1. Introduction

Hot star winds are highly supersonic, line-driven outflows whose mean properties are well-described by the current time-independent models (Kudritzki & Puls 2000). The line-driving mechanism itself is highly unstable, however, which should lead to shock heating of a small fraction of these winds to X-ray-emitting temperatures (Owocki, Castor, & Rybicki 1988; Feldmeier, Puls, & Pauldrach 1997). Because some O stars are relatively nearby and X-ray bright and because their winds are so fast, they are one of the few classes of sources for which *XMM-Newton* and *Chandra* can measure spectrally resolved line profiles. Such observations have the potential to provide the most direct diagnostics of the physical properties of the shocked winds of O stars, constraining the parameters of wind-shock theory as applied to the line-driven winds of hot stars.

Although the detailed description of the temperature, density, and velocity structure generated by the line-force instability in hot-star winds is undoubtedly complex and also currently open to debate, progress in understanding the X-ray production mechanism in hot stars can be made via the construction of simple, empirical models. Here we develop and present a simple, spherically symmetric model that includes a spatial distribution of X-ray emitting plasma, embedded within an absorbing wind. Our philosophy is to constrain parameters that describe the dynamics and spatial properties of the hot plasma embedded in the winds of these stars via a model that does not presuppose any particular physical model of shock generation and heating. Theorists can then test their specific physical models of X-ray production against the results of our empirical model fitting.

2. The Model

The model we will now describe and fit to data was developed by Owocki & Cohen (2001). It can be understood by first considering the emission from a uniform, optically thin, spherically expanding, constant velocity thin shell. Such a shell will lead to a broad, flat-topped line profile, with material in the front of the shell, moving toward the observer, accounting for the blue wing of the profile and material from the back of the shell, moving away from the observer, accounting for the red wing.

By summing over concentric shells, a model of a smooth, spherically expanding wind and its associated line profile can be developed. This is shown schematically in Fig. 1, where shells closer to the star, that are slower moving and denser, contribute narrower but higher flat-topped profiles and those that are farther from the star and moving faster contributer broader but lower flat-topped profiles. A smooth wind leads to a ta-

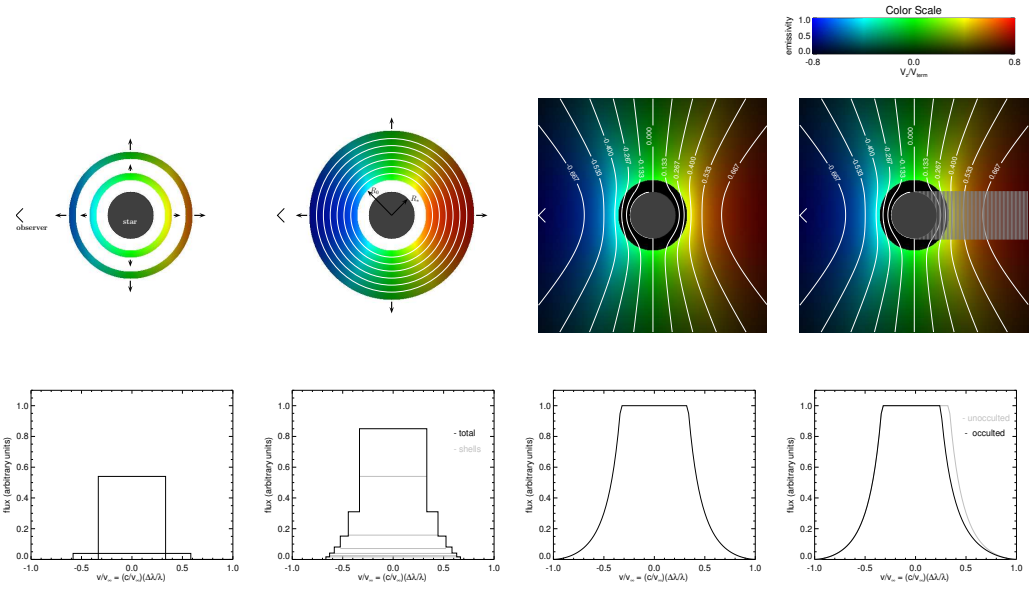

Figure 1. The development of a realistic, spherically symmetric wind model is shown in stages. The top, color panels show the distribution of X-ray emitting gas in the wind, with hue corresponding to line-of-sight velocity and saturation level corresponding to emissivity. The star itself is represented by the circle in the middle. Note that the model allows for the X-ray emitting plasma to be excluded from a region close from the star–hence the black gap between the star and the X-ray emitting wind. Lines of constant line-of-sight velocity are superimposed on the color scale in the latter two panels. Underneath each color panel is the corresponding line profile, shown in scaled velocity units (such that the terminal velocity corresponds to a value of unity). The first panel shows two spherical thin shells each with its own velocity, and each producing a box-shaped profile. The second panel shows a series of discrete, concentric shells. The third panel shows a smoothly changing, spherical wind, and the last panel includes the effects of occultation, which acts to break the symmetry.

pered profile, as shown in the third panel of the figure, having a flat top, corresponding to the innermost shell in the wind model, which can be assumed to be moving with some finite velocity that is less than the wind terminal velocity. The final panel in Fig. 1 shows that occultation by the star breaks the symmetry of the situation, leading to attenuation on the red side of the line profile, since the back of the wind is the redshifted portion and is also the portion that is occulted.

If we next consider attenuation by a cold, unshocked component of the wind, we get the situation shown in Fig. 2, where more of the red side of the line profile is removed. Because it is the emission from the back of the wind that suffers the most attenuation, the result of this effect is qualitatively like that of occultation, though in the case of wind absorption, some of the blue side of the profile can be attenuated if the wind is optically thick enough. Note that the resulting profiles have a characteristic skewed shape, with their peaks blueshifted and their blue wings much steeper than their red wings. We point out here that our assumption is that the individual sites of X-ray emission (assumed to be produced by individual shock waves) are so numerous, small, and evenly distributed throughout the wind that we can treat the wind as a two component fluid in which the bulk component is cold and X-ray absorbing, while a minor constituent is hot and X-ray emitting. We note further that the effects of continuum absorption on line profile shape have earlier been explored for thin shells (MacFarlane et al. 1991) and for a constant velocity spherical

outflow (Ignace 2001).

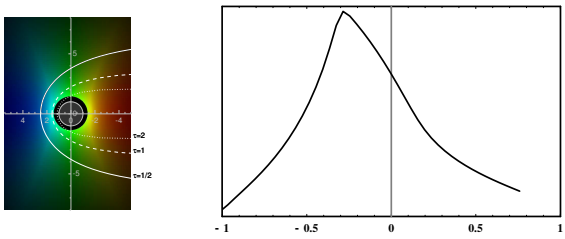

Figure 2. A model with attenuation by the cold wind. The representation shown on the left is the same as in Fig. 1, with the addition of contours of constant optical depth. The resulting line profile is shown on the right. Note the blueshift of the peak and the skewness of the profile due to the preferential absorption of red photons by the cold component of the wind.

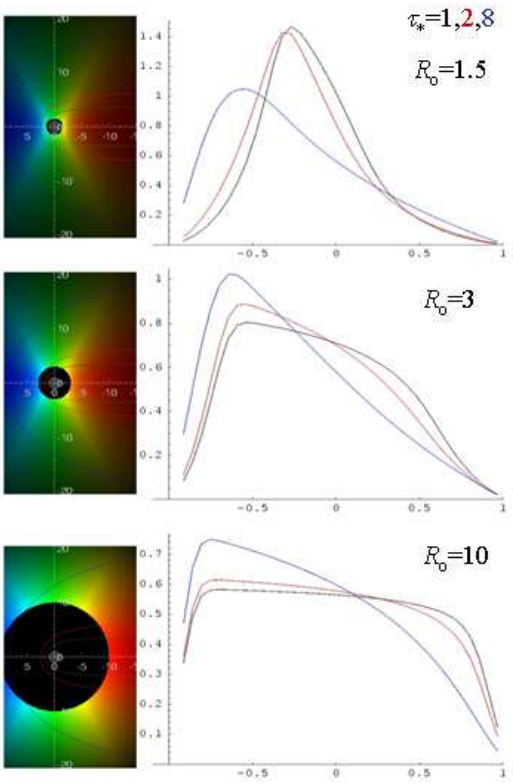

Figure 3. A series of synthetic line profiles is shown (along with the corresponding color contour plots of the wind structure; note that each panel has three different values of wind absorption (τ_*), with the three different optical depth unity contours indicated on each plot). It can be clearly seen that increasing the R_o parameter broadens the lines and makes them more box-like (looking from top to bottom), while increasing the degree of wind absorption (black, red, and blue on each panel) makes the lines somewhat broader, but primarily has the effect of increasing the blueshift and skewness of the profiles.

We characterize our model via four potentially adjustable parameters: R_o which is the radius at which the onset of X-ray production begins; q which is a power-law index describing the radial dependence of the X-ray filling factor (i.e., the fraction of the wind at a given radius that is in the hot, X-ray-emitting component); τ_* which describes the opacity of the cold component of the wind; and β which describes the wind acceleration (in the usual beta-velocity law) and is assumed to be the same for both components of the wind (the next refinement of our code will allow for different cold- and hot-wind β values). A complete mathematical description of these parameters and the equations governing the radiation transport appear in Owocki & Cohen (2001).

A suite of models having varying amounts of attenuation, and also having different spatial distributions of the X-ray-emitting plasma, are shown in Fig. 3. It can be seen from that figure that if broadened line profiles can be resolved by the new generation of X-ray telescopes, then the physical properties of the X-ray-emitting and absorbing winds can be constrained by fitting the data with the model we have described.

3. Fitting Data

We have performed such fits to six relatively strong and relatively unblended lines in the *Chandra HETGS* observation of the O4 supergiant ζ Pup, first reported on by Cassinelli *et al.* (2001). A more complete description of these data and the fitting results is available in Kramer, Cohen, & Owocki (2003). Our procedure is as fol-

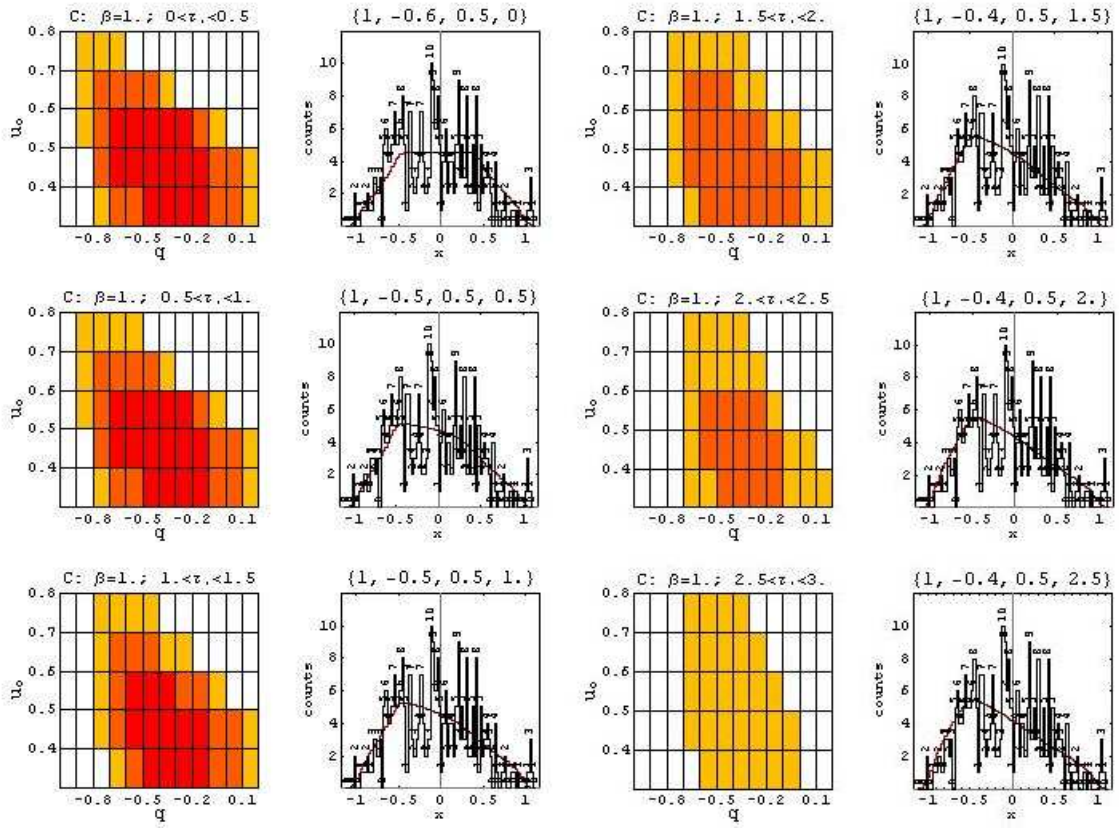

Figure 4. A series of panels showing a two-dimensional slice of the three-dimensional model parameter space (left, color panel) and the best-fit model *in that two-dimensional slice* in the right-hand panel, for a specific line. The value of τ_* is held constant in each slice, and increases from top to bottom and left to right. Note how the model profiles get more skewed with increasing τ_*. The color panels indicate the confidence limits at a set of discrete points in model parameter space. The red squares correspond to 68 % confidence boundaries, the orange to 95 %, and the yellow to 99 %.

lows: We first compute a large set of models in a three-dimensional volume on the R_o-q-τ_* parameter space (β is held constant at $\beta = 1$). We calculate the Cash C statistic for each individual model (Cash 1979), with the set of parameters giving the smallest C statistic value being the best-fit model. We then define confidence limits on this solution space based on the difference between the C statistic values for individual model realizations and the global best-fit value. Finally, we project the extremes of the confidence regions onto each of the three individual parameters in order to determine (jointly) the individual parameters' formal uncertainties.

We demonstrate this procedure graphically in Fig. 4, where we show two-dimensional slices of the three-dimensional model parameter space, along with the best-fit model from each two-dimensional slice superimposed on the data from one particular line. In Fig. 5 we demonstrate the range of parameters and resulting line profiles for one line, superimposing the best fit model as well as two models from opposite extremes of the τ_* dimension of parameter space on a measured line. The values of the model parameters are quite well constrained by the data (especially considering that we show 95 % confidence limits in both of these figures). More details of the

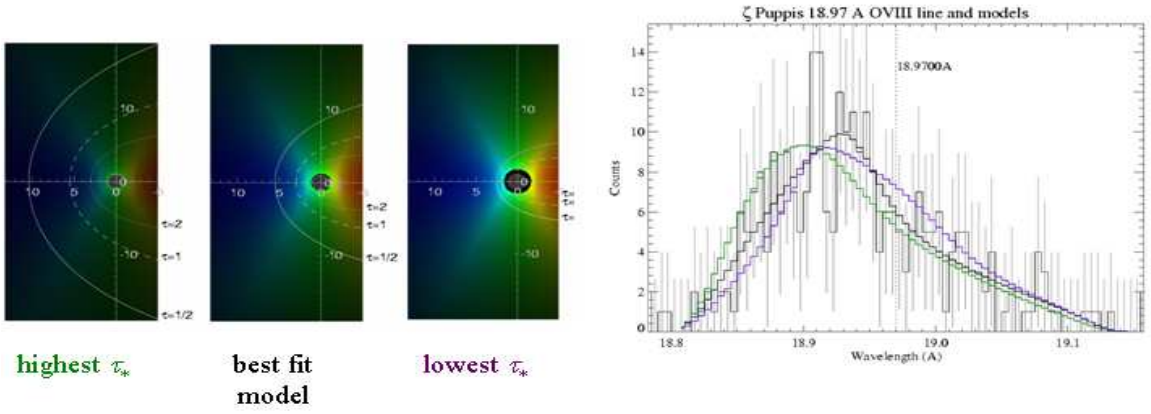

Figure 5. This figure demonstrates the limits that can typically be placed on the model parameters in a different way. We show the best-fit model for the oxygen Ly-α line along with two other models that are marginally consistent (at the 95 % level) with the data. These models represent the smallest and largest values of τ_* that are consistent with the data. The three color panels show the corresponding wind structure, in the same style as Figures 1, 2, and 3.

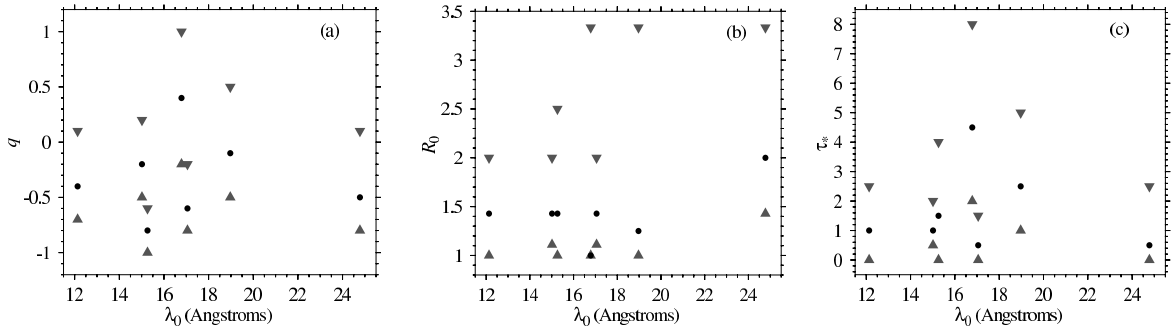

Figure 6. Summary of the best-fit wind parameters and confidence limits (q on the top, R_o in the middle, and τ_* on the bottom) for six of the lines we fit. The best-fit values are indicated by the black squares and the 95 % limits by the gray triangles.

model fitting, including the results of monte carlo simulations and a discussion of the goodness-of-fit assessment for each line are discussed in Kramer, Cohen, & Owocki (2003).

4. Results and Discussion

By the above-described procedure, we determine best-fit model parameters and formal uncertainties for each fitted line individually. The results for six lines are shown graphically in Fig. 6. The most notable result is that the X-ray emission lines observed with *Chandra* in this

star can, indeed, be fit by our simple spherically symmetric model. And, in fact, the results are broadly consistent with the expectations of line-driven instability wind-shock models (see, e.g., Owocki, Runacres, & Cohen 2000): The X-ray-emitting plasma is spatially distributed throughout the wind, above some small onset radius; The radial dependence of the X-ray filling factor is not strong; Attenuation by the cold, overlying wind plays an important role and strongly influences the observed X-rays.

However, there are several surprising results too. Chief among them is that the amount of wind attenuation determined from the fits to the lines is smaller than that which is expected given the mass-loss rate of ζ Pup. In fact, compared to the calculations in Hillier *et al.* (1993), we find a mean wind optical depth that is low by roughly a factor of five. Another, and possibly related, result is that there is little if any trend in derived model parameters from line to line. This is true of the derived values of τ_*, which one would expect to vary strongly with wavelength, reflecting the dependence of photoionization cross sections on wavelength.

One possible explanation for these two surprising results is wind clumping. If the absorbing component of the wind is very inhomogeneous, then the wind will be effectively porous, allowing more photons to escape and lowering the mean wind optical depth. Such clumpiness in the cold wind component might also affect the independent determinations of the mass-loss rates of hot stars. This effect would serve to reduce the mass-loss rates and hence the expected wind optical depths, thus acting in concert with the porosity of the wind to bring our observations and derived parameters more in line with expectations.

Wind clumping, if extreme, may also help explain the lack of wavelength dependence of the derived τ_* values. If clumps are individually optically thick, then the geometric cross sections of clumps governs the mean wind opacity, rather than the (wavelength-dependent) atomic cross sections. It is possible, however, that because the lines we fit cover only a relatively small range of wavelengths, that the ionization balance in the cold wind component and the wavelength distribution of K-shell edges could conspire to significantly flatten the wavelength dependence of the wind opacity.

Finally, the lack of any strong dependence of the other two parameters (R_o and q) on the line being fit seems to indicate that the various temperature components of the X-ray-emitting plasma, which produce the different observed lines, have a relatively uniform spatial distribution throughout the wind.

In summary, the analysis of X-ray line profiles provides a lot of information about the dynamics and inferred geometry of the hot plasma embedded in the winds of O stars, as well as on the nature of the cold, X-ray absorbing winds of these objects. For ζ Pup, some type of wind-shock mechanism is favored. For other O and B stars observed thus far with *Chandra* and *XMM-Newton* , however, relatively narrow or symmetric emission lines indicate that our simple, spherically symmetric wind-shock model may not be a good description of the observed X-rays.

REFERENCES

1. Cash, W. 1979, ApJ, 228, 939
2. Cassinelli, J. P., Miller, N. A., Waldron, W. L., MacFarlane, J. J., & Cohen, D. H. 2001, ApJ, 554, L55
3. Feldmeier, A., Puls, J., & Pauldrach, A. W. A. 1997, A&A, 322, 878
4. Hillier, D. J., Kudritzki, R. P., Pauldrach, A. W., Baade, D., Cassinelli, J. P., Puls, J., & Schmitt, J. H. M. M. 1993, ApJ, 276, 117
5. Kramer, R. H., Cohen, D. H., & Owocki, S. P. 2003, ApJ, in press
6. Kudritzki, R.-P., & Puls, J. 2000, ARA&A, 38, 613
7. Ignace, R. 2001, ApJ, 549, L119
8. MacFarlane, J. J., Cassinelli, J. P., Welsh, B. Y., Vedder, P. W., Vallerga, J. V., & Waldron, W. L. 1991, ApJ, 380, 564
9. Owocki, S. P., Castor, J. I., & Rybicki, G. B. 1988, ApJ, 335, 914
10. Owocki, S. P., & Cohen, D. H. 2001, ApJ, 559, 1108
11. Owocki, S. P., Runacres, M. C., & Cohen, D. H. 2000, ASP Conf. Ser. 204, ed. Lamers & Sapar, p. 183

ACKNOWLEDGEMENTS

RHK wishes to acknowledge the Howard Hughes Medical Institute summer research grant from Swarthmore College. DHC and SPO acknowledge NASA grant NAG 5-3530.